Journal of Magnetic Resonance **139,** 225–231 (1999)
Article ID jmre.1999.1781, available online at http://www.idealibrary.com on IDEAL®

Consequences of ^{129}Xe–^{1}H Cross Relaxation in Aqueous Solutions

Andrea Stith,* T. Kevin Hitchens,† Denise P. Hinton,† Stuart S. Berr,‡ Bastiaan Driehuys,§ James R. Brookeman,*,‡ and Robert G. Bryant*,†

*Biophysics Program, †Department of Chemistry, ‡Departments of Radiology and Biomedical Engineering, University of Virginia, Charlottesville, Virginia 22901; and §Magnetic Imaging Technologies, Inc., 2500 Meridian Parkway, Suite 175, Durham, North Carolina 27713

Received June 19, 1998; revised April 9, 1999

We have investigated the transfer of polarization from ^{129}Xe to solute protons in aqueous solutions to determine the feasibility of using hyperpolarized xenon to enhance ^{1}H sensitivity in aqueous systems at or near room temperatures. Several solutes, each of different molecular weight, were dissolved in deuterium oxide and although large xenon polarizations were created, no significant proton signal enhancement was detected in L-tyrosine, α-cyclodextrin, β-cyclodextrin, apomyoglobin, or myoglobin. Solute-induced enhancement of the ^{129}Xe spin–lattice relaxation rate was observed and depended on the size and structure of the solute molecule. The significant increase of the apparent spin–lattice relaxation rate of the solution phase ^{129}Xe by α-cyclodextrin and apomyoglobin indicates efficient cross relaxation. The slow relaxation of xenon in β-cyclodextrin and L-tyrosine indicates weak coupling and inefficient cross relaxation. Despite the apparent cross-relaxation effects, all attempts to detect the proton enhancement directly were unsuccessful. Spin–lattice relaxation rates were also measured for Boltzmann ^{129}Xe in myoglobin. The cross-relaxation rates were determined from changes in ^{129}Xe relaxation rates in the α-cyclodextrin and myoglobin solutions. These cross-relaxation rates were then used to model ^{1}H signal gains for a range of ^{129}Xe to ^{1}H spin population ratios. These models suggest that in spite of very large ^{129}Xe polarizations, the ^{1}H gains will be less than 10% and often substantially smaller. In particular, dramatic ^{1}H signal enhancements in lung tissue signals are unlikely. © 1999 Academic Press

Key Words: **xenon; α-cyclodextrin; nuclear Overhauser effect; optical pumping; cross relaxation.**

INTRODUCTION

^{129}Xe nuclear spin populations attain significant population differences by optical pumping methods and the resulting gain in sensitivity can approach five orders of magnitude (*1*). This increased sensitivity makes magnetic resonance imaging of cavities such as lung (*2–12*) and dissolved phase tissue studies (*13, 14*) possible. In addition to the direct detection of the hyperpolarized nucleus, the transfer of polarization may allow for the signal enhancement of secondary nuclei. At modest or high magnetic fields, nuclei may cross-relax via the nuclear Overhauser effect (NOE) despite different resonance frequencies (*15*). Successful transfer will make possible the study of nuclear spins on biologically significant molecules in aqueous solutions for which NMR studies may be limited by sensitivity.

Pines and co-workers have successfully demonstrated Overhauser effects from hyperpolarized ^{129}Xe to ^{1}H in 25% C_6D_5H dissolved in deuterobenzene (*16*). The ^{1}H spin–lattice relaxation time was long and despite the small transfer rate, there was a detectable increase of the dilute ^{1}H spin polarization. Pines and co-workers have also reported a small ^{1}H signal enhancement in 100 mM α-cyclodextrin dissolved in d_6-dimethyl sulfoxide using a difference SPINOE pulse sequence (*17*). The solubility of xenon in this nonaqueous solvent is significantly increased and as a result, the polarized xenon spin pool is much larger and the amplification of the proton signal more clearly detectable.

In this report, we examine cross relaxation and the increase of ^{1}H polarization of several macromolecules in aqueous (D_2O) solution. The choice of an aqueous solution is significant, because we are interested in the extension of this technique to the observation of solute molecules in water as well as *in vivo* magnetic resonance spectroscopy and imaging. We have used a procedure similar to that of Pines and co-workers (*17*) to examine proton-rich solute molecules, some of which bind xenon specifically. With the exception of some of the myoglobin studies, where interaction with the macromolecule principally dominated ^{129}Xe relaxation, D_2O was used to minimize water proton-induced xenon spin–lattice relaxation.

RESULTS

The final polarization level of ^{129}Xe gas is a function of the accumulated volume of gas, the gas flow rate, and the accumulation time (*18–21*). In these experiments, the xenon polarization was estimated to be 2–3% in the sample bulb. This value was determined in two ways. First, we compared the hyperpolarized xenon gas peak to the peak of Boltzmann level xenon dissolved in octanol. Second, we compared the hyperpolarized xenon gas peak to the signal of the same gas sample after being allowed to relax, unperturbed, in the magnet overnight. The T_1 of the gas in the surface-treated sample bulbs was generally in excess of 1 h. While the intensity measurements

1090-7807/99 $30.00

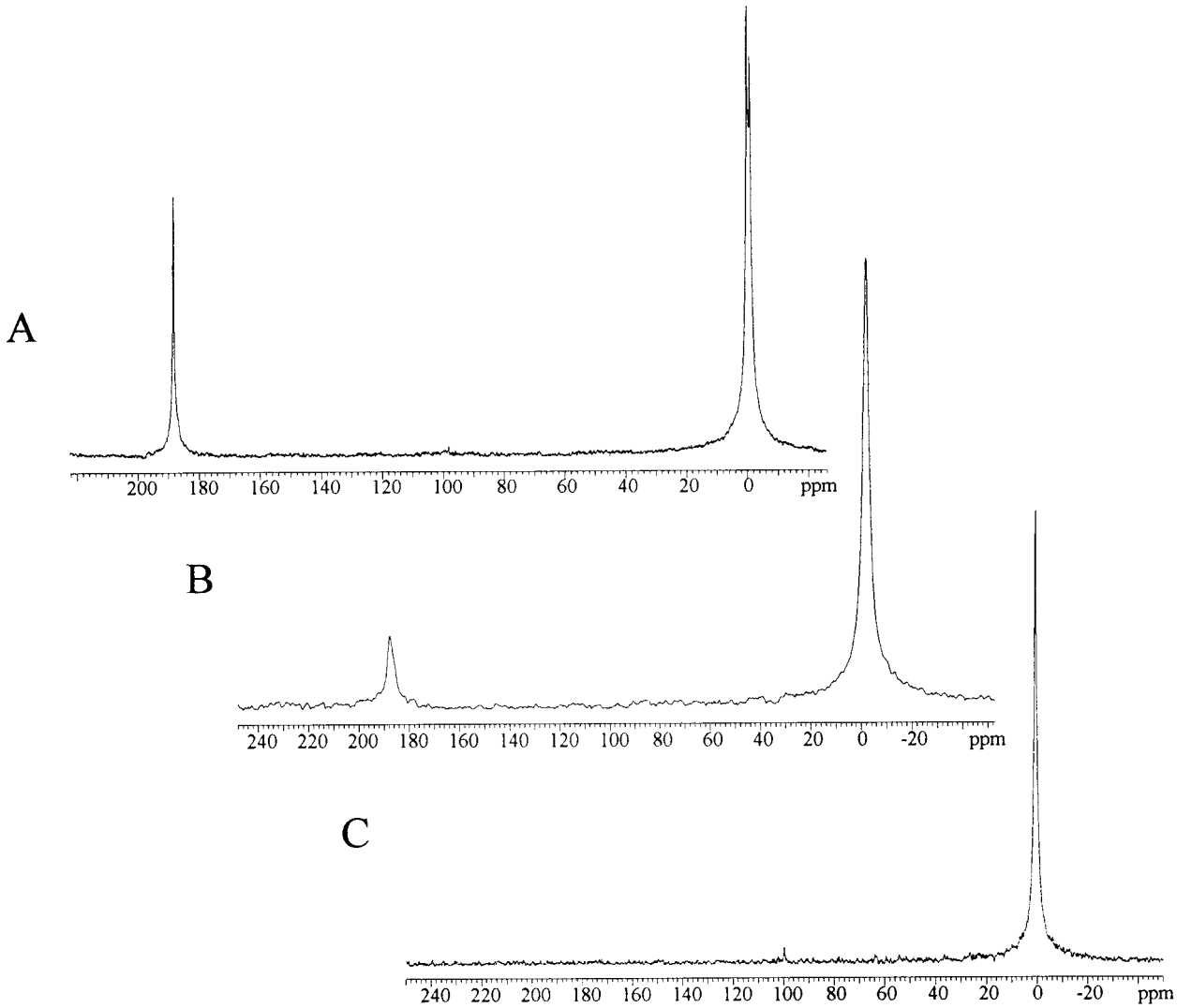

FIG. 1. ^{129}Xe NMR spectra recorded at 55.347 MHz and ambient laboratory temperature for solutions of (A) 10 mM β-cyclodextrin, (B) 10 mM α-cyclodextrin, and (C) 5 mM apomyoglobin in deuterium oxide. The gas phase resonance is set to 0 ppm, and the initial ^{129}Xe polarization is on the order of a few percent. The time required to mix the sample, position it in the magnet, and begin acquisition is approximately 10 s. The differences in dissolved phase resonances (at approximately 190 ppm) are attributed to variance in cross-relaxation rates for ^{129}Xe with each of the solute protons.

themselves are not a particular problem, errors may accumulate because of very different attenuator settings required in the comparison, pulse width calibration errors, which are amplified greatly by the scaling factors required for the comparison, and sampling artifacts that may include differences in surface-induced relaxation rates in the different containers used for the hyperpolarized samples. Nevertheless, the polarization obtained is very substantial and represents approximately a 3000 fold gain over the equilibrium magnetization. T_1 measurements for hyperpolarized samples were made by repeated single acquisitions with a small flip angle. For these measurements, the sampling RF pulses dominate the xenon signal decrease. The T_1 of hyperpolarized ^{129}Xe dissolved in D_2O at 4.7 T is 470 s. For the Boltzmann ^{129}Xe studies, the T_1 measurements were made with a saturation-recovery pulse sequence. The T_1 measurement of ^{129}Xe at Boltzmann equilibrium was determined to be 592 $\pm$ 37 s at 11.7 T. Consistent with previous studies, we have found the T_1 values to be shortened by interactions with dissolved oxygen (*22*, *23*) and collisions with uncoated glassware walls (*24*, *25*). Nonetheless, the long relaxation time in D_2O allows considerable opportunity for the relaxation coupling of ^{129}Xe to ^{1}H of the solute molecule.

Figures 1A, 1B, and 1C show the gas and dissolved phase resonances for ^{129}Xe in the β-cyclodextrin, α-cyclodextrin, and apomyoglobin samples, respectively. For each, the free xenon concentration was assumed to be 4.3 mM. The delay between rapid mixing of the gas/water sample and spectral acquisition was consistent at 10 s for each sample. Thus, the differences in dissolved ^{129}Xe peak amplitude may be attributed to relaxation effects. The slow decay of the xenon resonance in aqueous

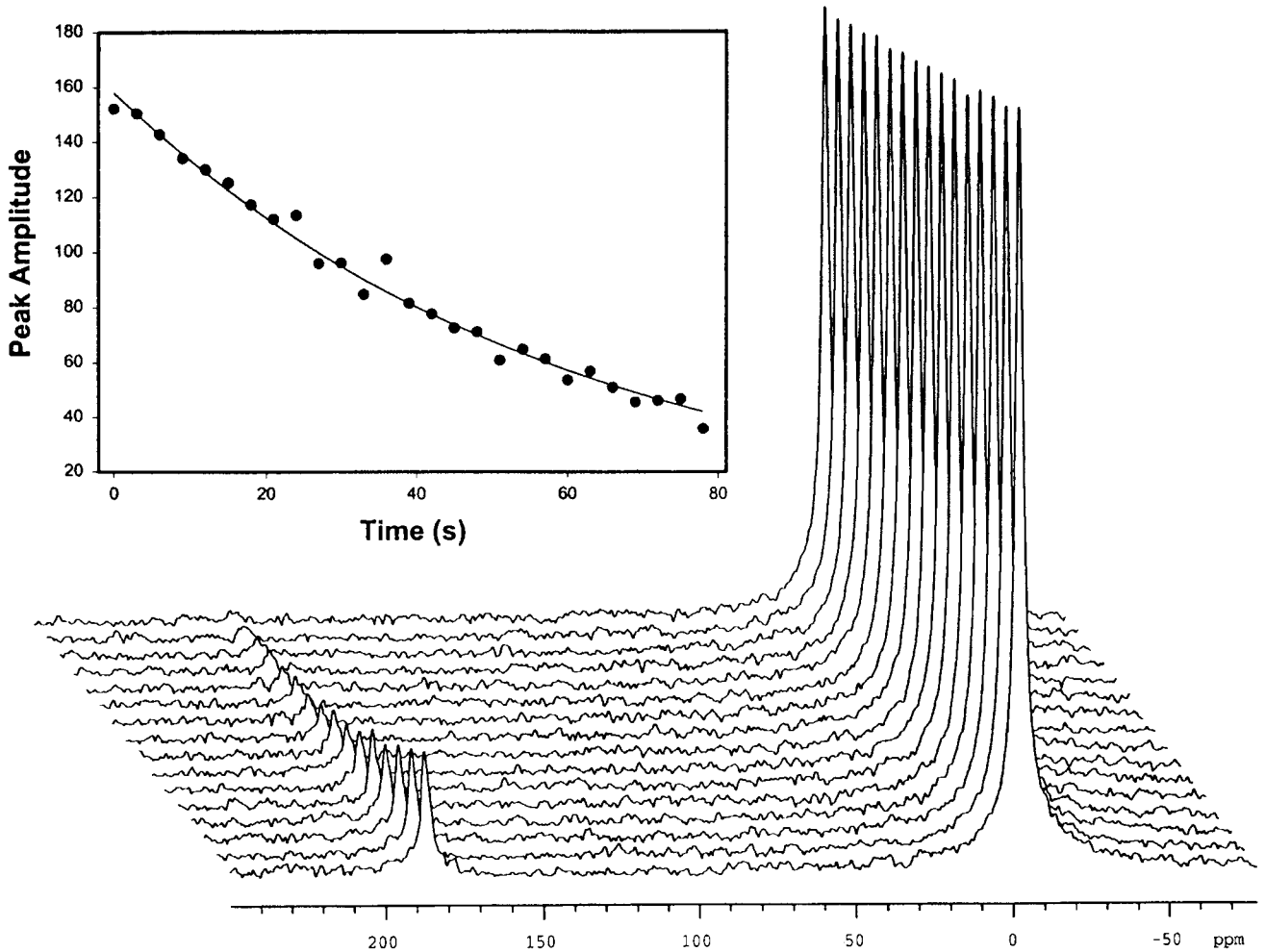

FIG. 2. ^{129}Xe NMR spectra shown in a stacked plot recorded at 55.347 MHz at ambient laboratory temperature for 10 mM α-cyclodextrin in deuterium oxide. The dissolved phase is at 190 ppm relative to the gas phase. Single transients were recorded using 12° pulses every 3 s. The inset plot is an exponential fit to the dissolved xenon resonance intensity with an apparent time constant of 106 s, taking into account the effects of the successive sampling pulses.

solutions of 10 mM β-cyclodextrin demonstrates weak coupling between the xenon and the solute protons, and is consistent with the absence of specific complex formation. The increased relaxation of dissolved xenon in the α-cyclodextrin solution is characteristic of the formation of a host–guest complex and an efficient relaxation pathway. The relaxation of xenon in a 10 mM solution of α-cyclodextrin dissolved in D_2O is shown in Fig. 2 as a series of ^{129}Xe spectra as a function of time. The observed T_1, corrected for the decay as a result of the sampling pulses, is 105 $\pm$ 2 s. The lack of dissolved phase signal in Fig. 1C is due to rapid relaxation of the dissolved xenon which specifically binds to diamagnetic apomyoglobin. The reported rate constant for xenon exchanging with the binding sites of myoglobin is 2×10^7 M^{-1} s^{-1} for the native protein (*26*). This rapid exchange provides sufficiently efficient relaxation paths for the xenon spins such that no signal from dissolved hyperpolarized xenon was detected after the mixing period. The spin–lattice relaxation time measured for ^{129}Xe at thermal equilibrium in a 0.1 mM aqueous solution of myoglobin was 1.3 s at 4.7 T and confirms that the protein binding sites provide an efficient relaxation pathway for xenon.

^{1}H signal enhancement was also examined for these solutes of different molecular weight. Regardless of the proton-induced enhancement of the ^{129}Xe relaxation rate, no significant increase in the ^{1}H signal intensity was observed for any solute studied within experimental error of single-pulse ^{1}H acquisitions.

DISCUSSION

We may characterize the efficiency of cross relaxation by examining the proton contribution to the apparent xenon spin–lattice relaxation rate. Following Solomon (*15*),

$$\frac{d\langle I_Z\rangle}{dt} = -(\rho_{II} + \rho_{IS})(\langle I_Z\rangle - I_0) - \sigma_{IS}(\langle S_Z\rangle - S_0)$$

$$\frac{d\langle S_Z\rangle}{dt} = -(\rho_{SS} + \rho_{SI})(\langle S_Z\rangle - S_0) - \sigma_{SI}(\langle I_Z\rangle - I_0), \quad [1]$$

where S is identified with the xenon spin and I with the proton spin. ρ_{II} and ρ_{SS} are contributions to the spin–lattice relaxation rate from like-spin couplings, and ρ_{SI} and ρ_{IS} are spin–lattice relaxation contributions from unlike spins. Because the concentration of xenon is low, both proton relaxation and xenon relaxation are dominated by interactions with solute protons. Therefore, both ρ_{IS} and ρ_{SS} are neglected. Noting that we are in the short correlation time limit and following the argument outlined in (*16*), we find

$$\sigma_{SI} = \left[\frac{S(S+1)}{2I(I+1)}\right]\rho_{SI}. \quad [2]$$

At equilibrium, the cross-relaxation rates R_{IS} and R_{SI} must be equal. Because of detailed balance, we may write

$$S(S+1)\,N_I\sigma_{IS} = I(I+1)\,N_S\sigma_{SI}, \quad [3]$$

where N_S and N_I are the numbers of xenon and proton spins, respectively. Substituting Eq. [2] into Eq. [3] and assuming that the xenon spin–lattice relaxation rate is dominated by the cross relaxation to the protons yield

$$\sigma_{IS} = \frac{N_S}{2N_I}\frac{1}{T_{1Xe}}. \quad [4]$$

Thus, the measurement of ^{129}Xe T_1 in α-cyclodextrin solutions provides a measurement of the cross-relaxation rate to protons. Assuming that the water is saturated with xenon (4.3 mM) we may compute the concentration of xenon bound to the α-cyclodextrin cavity. Bartik and co-workers (*27*) and Hitchens and Bryant (*28*) have shown that xenon binds to α-cyclodextrin with an equilibrium constant of 16–20 M^{-1}. Thus, binding in the α-cyclodextrin cavity provides a site for relatively strong ^{129}Xe–^{1}H coupling that reduces the net xenon relaxation time substantially. The fast exchange limit of the relaxation equation is appropriate and we may compute the relaxation rate for the bound environment. The deuterium exchange with the OH groups of α-cyclodextrin eliminated some short distance proton–xenon contributions to the overall coupling. Thus, there are 7 remaining protons on each sugar (42 protons per molecule) that may interact with the bound xenon. Using Eq. [4] we obtain $\sigma_{SI} = 1.2 \times 10^{-5}\ s^{-1}\ mM^{-1}$. This cross-relaxation rate is the sum over the cross-relaxation rates to each proton. Pines and collaborators have measured proton signal enhancements in dimethyl sulfoxide solutions of α-cyclodextrin and report cross-relaxation rates for each proton (*17*). We compute the relevant sum from their data as $1.5 \times 10^{-5}\ s^{-1}\ mM^{-1}$, which is in fair agreement with the value determined from this study.

The spectrum of hyperpolarized ^{129}Xe in aqueous (D_2O) 4 mM myoglobin solutions was not detectable using the mixing and acquisition methods of these experiments at 4.7 T. Measurements of the xenon T_1 at 4.7 T using only the perturbations of the ^{129}Xe magnetization at thermal equilibrium in 0.1 mM myoglobin solutions returned an average value of 1.3 ± 0.2 s. At the same concentrations, the ^{129}Xe resonance was not reliably detected at 11.7 T. Experiments at 11.75 T using Boltzmann equilibrium ^{129}Xe populations and a variety of protein solutions including myoglobin have demonstrated that xenon resonances may be very broad and sometimes undetectable. This problem was solved in part by reducing the protein concentration and lowering the magnetic field strength. In the earlier work of Tilton and Kuntz (*26*) on myoglobin and hemoglobin solutions, the temperature dependence of the xenon resonance implied that the chemical shift difference between the myoglobin sites and the aqueous pool is on the order of 40 ppm. The chemical exchange of the xenon with the aqueous pool then makes the Larmor frequency time dependent. They used the simplified equation

$$\Delta\nu = P_A(1 - P_A)^2 4\pi(\Delta\nu_{AB})^2\tau_{bound}, \quad [5]$$

where $\Delta\nu$ is the full width at half-height, P_A is the probability that the xenon is not bound, $\Delta\nu_{AB}$ is the chemical shift between the bound and unbound environment expressed in hertz, and τ_{bound} is the mean lifetime in the bound environment. Because the chemical shift is linear in the magnetic field strength, the exchange contribution to the broadening increases as the square of the field strength. Resonances readily detected at 1.5 T may be hundreds of hertz wide at higher field strengths. Because *in vivo* environments will present a distribution of xenon macromolecule binding sites and lifetimes, we may anticipate a distribution of linewidth contributions that is strongly dependent on magnetic field strength. In some instances at high fields, the time-dependent chemical shift caused by chemical exchange events may make the xenon resonance impracticably broad for routine observation.

Myoglobin has two binding sites for xenon characterized by association constants of 190 and 10 M^{-1} (*26*). A treatment parallel to that used for α-cyclodextrin may yield an effective average xenon–proton cross-relaxation rate. At the low concentrations used in our experiments, the weak binding site makes a very small contribution to the total bound state concentration and may be neglected. N_H is ambiguous because it may include not only those protons in van der Waals contact with the xenon in the binding site, but also other spins which are in contact with the xenon through spin diffusion. Without precise knowledge of the number of protein protons that effectively interact with the xenon nucleus over the time course of the observation, quantitative deductions are limited. The

TABLE 1
Myoglobin Cross-Relaxation Parameters

	N_H				
	5	10	50	100	1000
σ_{Xe-H} (mM^{-1} s^{-1})	0.76	0.38	0.077	0.038	0.0038

Note. ^{129}Xe–^{1}H computed cross-relaxation rates for different populations of ^{1}H spins because the number of ^{1}H spins in the xenon binding pocket is not known precisely. These cross-relaxation rates are calculated given $T_{1Xe} = 1.3$ s and $K = 190$ M^{-1}.

effective size of the relevant proton population may range from the order of 10 protons to many more, depending on the details of local structure and dynamics within the protein–protein spin system. Therefore, we have computed an array of cross-relaxation rates that are dependent on the choice of the effective ^{1}H spin pool size. These rates, summarized in Table 1, are all substantially larger than those measured for α-cyclodextrin. This increase in ^{129}Xe–^{1}H cross-relaxation rate may be explained by an increased correlation time, an increased number of proton spins, or a decreased effective internuclear distance. The greater cross-relaxation efficiency is consistent with the larger rotational correlation time for motion of the protein compared with α-cyclodextrin. The protein binding sites will generally have fewer exchangeable protons than the hydroxyl-rich sugars of α-cyclodextrin; thus, the binding site region in the protein is probably richer in ^{1}H spins, which will increase the cross-relaxation rate.

Figure 3 shows the calculated prediction of the effect of ^{129}Xe cross relaxation on the ^{1}H magnetization. The ^{1}H T_1 is assumed to be 1 s, the ^{129}Xe relaxation rate is 0.002 s^{-1}, and the cross-relaxation rate constant is 1.2×10^{-5} mM^{-1} s^{-1}. The curves predict the ^{1}H magnetization for various ratios of ^{129}Xe–^{1}H population ratios (N_S/N_I) based on the solution of Eqs. [1]. The top curve is the predicted magnetization enhancement for ^{1}H spins in the 10 mM α-cyclodextrin experiments and the bottom curve is representative of ^{1}H spin populations *in vivo.* These calculations show that the spin population ratio affects not only the maximum magnetization enhancement but also the apparent lifetime of the ^{1}H magnetization enhancement. For the α-cyclodextrin experiments this model predicts a 3.5% average increase in the intensity of each ^{1}H resonance line and the magnetization will remain near this level for more than 10 s. However, in the bottom curve, the maximum enhancement is just over 1.0% and dissipates in less than 6 s.

We note that there is a crucial difference between the total proton magnetization enhancement and the magnetization enhancement detectable in a particular resonance. The signal increase in a particular resonance line, which is relevant for spectroscopic studies, is generally only a fraction of the total proton population enhancement. The total ^{1}H population enhancement may be much larger and is conceivably detectable in an imaging experiment. The ^{1}H enhancement may be improved if the size of the hyperpolarized xenon pool were increased; however, in water, xenon solubility may set a practical limit. Thus, spectral enhancements in the context of high-resolution experiments in water at convenient pressures and temperatures are expected to be modest at best.

CONCLUSIONS

These measurements of xenon relaxation demonstrate that the xenon spin–lattice relaxation rate is not a limiting factor in determining the proton signal enhancement in experiments that depend on the Overhauser effect to pump the proton intensity. Although obtained by different means the cross-relaxation rates between the xenon and protons in α-cyclodextrin are in agreement with the values reported by Navon *et al.* (*16*). The small xenon–proton cross-relaxation rate, in combination with significant proton spin–lattice relaxation, limit the intensity of the proton signal enhancement obtainable from contact with a hyperpolarized xenon population. In addition, the proton concentration in tissue systems is high and the aqueous xenon solubility limited, so detectable proton signal enhancements are expected to be small and provide limited opportunities for *in vivo* application to proton spectroscopy and imaging. Finally, time-dependent chemical shifts caused by chemical exchange among xenon binding environments provide a significant line broadening mechanism that may make xenon linewidths very broad at high magnetic field strengths.

EXPERIMENTAL

^{129}Xe was polarized via spin exchange with optically polarized rubidium (Rb) vapor, utilizing the high-volume method

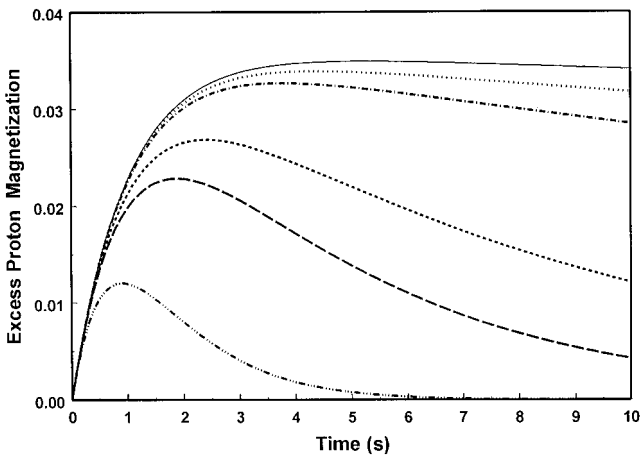

FIG. 3. Computed reduced magnetization for different choices of relative ^{129}Xe to ^{1}H population ratios. The values for T_1^H, T_1^{Xe}, and σ_{IS} are 1 s, 470 s, and 1.2×10^{-5} mM^{-1} s^{-1}, respectively. The xenon polarization was approximately 3%. From top to bottom, the parameters for the population ratio, N_S/N_I, are 0.003, 0.001, 0.005, 0.0001, 0.00005, and 0.000001.

for producing laser-polarized ^{129}Xe (*29*). A 100-W laser diode array centered at 795 nm was used to excite the D1 absorption resonance of Rb. Approximately 10 atm of ^{4}He was used to broaden the rubidium absorption, while only about 0.1 atm of ^{129}Xe was present. At 420 K, using this mixture of gas, the Rb–Xe spin exchange time is 22 s and the use of a continuous flow of gas is possible. Specifically, this system uses a 10-atm gas mixture that is approximately 98% ^{4}He, 1% Xe, and 1% N_2 (Isotec, Inc. Miamisburg, OH) that flows through the optical pumping chamber so that a given xenon atom spends one to two spin exchange periods in contact with the polarized Rb vapor. The hyperpolarized xenon gas is extracted by trapping it in a cold finger surrounded by liquid nitrogen. In suitable circumstances, the polarization is substantially retained during the freezing process and a long spin–lattice relaxation time of ^{129}Xe at 77 K (approximately 3 h) makes the storage of the polarized gas possible (*30*). For early experiments, accumulations occurred over 1–2 h with several liters of hyperpolarized gas allocated to several vials. In the later applications, hyperpolarized xenon was accumulated for each experiment over a period of 10–15 min. In some experiments, the xenon used was enriched to 71% ^{129}Xe (Urenco, Almelo, The Netherlands). For the bulk of the experiments, natural abundance (26.44% ^{129}Xe) xenon samples were used (Spectra Gases, Alpha, NJ). When an accumulation run was finished, the frozen xenon was vaporized and collected in the sample vial for transport to the NMR spectrometer.

Nuclear magnetic resonance measurements were made at 4.7 T at ambient laboratory temperature in a 40-cm horizontal-bore imaging magnet using a Varian SIS 200/400 spectrometer system. All glassware in contact with hyperpolarized xenon was treated with 10% solution of dichlorodimethylsilane in hexane, and then rinsed with methanol and evacuated to ensure removal of residual solvent. The D_2O solutions were introduced by syringe through a rubber septum and the small hole in the glass stopcock and the sample was vigorously shaken and placed into the Rf coil and magnet and acquisition was started immediately using small flip angles ($<20°$) to detect ^{129}Xe or ^{1}H resonances. ^{129}Xe spin–lattice relaxation time measurements were also made on samples initially at thermal equilibrium using the 4.7-T instrument or on an 11.7-T Varian Unity Plus NMR spectrometer. The 11.7-T measurements used a 10-mm broadband probe tuned to 138 MHz and 10-mm NMR tubes treated with dichlorodimethylsilane as previously described. T_1 measurements with Boltzmann samples were made using a saturation-recovery pulse sequence.

L-Tyrosine was obtained from Fisher Scientific, α-cyclodextrin and β-cyclodextrin were from Aldrich, and horse skeletal myoglobin was from Sigma Chemical Co. The labile protons of α- and β-cyclodextrin were out exchanged by three lyophilization cycles from D_2O. Solutions were in D_2O at 10, 10, and 5 mM for α-cyclodextrin, β-cyclodextrin, and L-tyrosine, respectively. Apomyoglobin was prepared by standard methods and the resulting protein was faintly yellow (*31*). Both myoglobin and apomyoglobin were lyophilized from three successive D_2O solutions to minimize the proton concentration in the final solution. For the studies of hyperpolarized ^{129}Xe and apomyoglobin and myoglobin, the nominal protein concentrations were 4 mM. For studies done with Boltzmann ^{129}Xe and myoglobin, the protein was dissolved in water at a concentration of 100 μM.

ACKNOWLEDGMENTS

This work was supported by the National Institutes of Health under Grant GM34541 and the University of Virginia. We thank Melinda Whaley Hodges for preparing the apomyoglobin and Professor Gordon Cates for helpful discussions. We also appreciate conversations with Professors Gil Navon and Alex Pines, and Scott Swanson. We also thank Dr. Jack Knight-Scott, Therese Maier, and Vu Mai for technical assistance and Jaime Mata for polarizing the gas.

REFERENCES

1. W. Happer, E. Miron, S. Schaefer, D. Schreiber, W. A. Van Wijngaarden, and X. Zeng, Polarization of the nuclear spins of noble-gas atoms by spin exchange with optically pumped alkali-metal atoms, *Phys. Rev. A* **29,** 3092 (1984).
2. M. S. Albert, G. D. Cates, B. Driehuys, W. Happer, B. Saam, C. S. Springer, Jr., and A. Sishnia, Biological magnetic resonance imaging using laser-polarized ^{129}Xe, *Nature* **370,** 199–201 (1994).
3. H. Middleton, R. D. Black, B. Saam, G. D. Cates, G. P. Cofer, R. Guenther, W. Happer, L. W. Hedlund, G. A. Johnson, K. Juvan, and J. Swartz, MR imaging with hyperpolarized ^{3}He gas, *Magn. Reson. Med.* **33,** 271–275 (1995).
4. R. D. Black, H. L. Middleton, G. D. Cates, G. P. Cofer, B. Driehuys, W. Happer, L. W. Hedlund, G. A. Johnson, M. D. Shattuck, and J. C. Swartz, In vivo ^{3}He images of guinea pig lungs, *Radiology* **199,** 867–870 (1996).
5. M. S. Albert, C. H. Tseng, D. Williamson, E. R. Oteiza, R. L. Walsworth, B. Kraft, D. Kacher, B. L. Holman, and F. A. Jolesz, Hyperpolarized ^{129}Xe MR imaging of the oral cavity, *J. Magn. Reson. B* **111,** 204–207 (1996).
6. J. R. Macfall, H. C. Charles, R. D. Black, H. Middleton, J. C. Swartz, B. Saam, B. Driehuys, C. Erickson, W. Happer, G. D. Cates, G. A. Johnson, and C. E. Ravin, Human lung air spaces: Potential for MR imaging with hyperpolarized He-3, *Radiology* **200,** 553–558 (1996).
7. K. Sakai, A. M. Bilek, E. Oteiza, R. L. Walsworth, D. Balamore, F. A. Jolesz, and M. S. Albert, Temporal dynamics of hyperpolarized ^{129}Xe resonances in living rats, *J. Magn. Reson. B* **111,** 300–304 (1996).
8. M. E. Wagshul, T. M. Button, H. F. Li, Z. Liang, C. S. Springer, Jr., K. Zhong, and A. Wishnia, In vivo MR imaging and spectroscopy using hyperpolarized ^{129}Xe, *Magn. Reson. Med.* **36,** 183–191 (1996).
9. P. Bachert, L. R. Schad, M. Bock, M. V. Knopp, M. Ebert, T. Grossmann, W. Heil, D. Hofmann, R. Surkau, and E. W. Otten, Nuclear magnetic resonance imaging of airways in humans with use of hyperpolarized ^{3}He, *Magn. Reson. Med.* **36,** 192–196 (1996).
10. H. U. Kauczor, D. Hofmann, K. F. Kreitner, H. Nilgens, R. Surkau, W. Heil, A. Potthast, M. V. Knopp, E. W. Otten, and M. Thelen, Normal and abnormal pulmonary ventilation: Visualization at hyperpolarized He-3 MR imaging, *Radiology* **201,** 564–568 (1996).
11. J. R. Brookeman, J. P. Mugler III, P. Bogorad, T. M. Daniel, E. E. De Lange, B. Driehuys, J. Knight-Scott, T. Maier, J. D. Truwit, G. Cates, and W. Happer, Polarized noble gas MRI, *in* "Polarized Gas

Targets and Polarized Beams: Seventh International Workshop" (R. J. Holt and M. A. Miller, Eds.) (1998).

12. J. P. Mugler III, B. Driehuys, J. R. Brookeman, G. D. Cates, S. S. Berr, R. G. Bryant, T. M. Daniel, E. E. De Lange, J. H. Downs III, C. J. Erickson, W. Happer, D. P. Hinton, N. F. Kassel, T. Maier, C. D. Phillips, B. T. Saam, K. L. Sauer, and M. E. Wagshul, MR imaging and spectroscopy using hyperpolarized ^{129}Xe gas: Preliminary human results, *Magn. Reson. Med.* **37,** 809–815 (1997).
13. S. D. Swanson, M. S. Rosen, B. W. Agranoff, K. P. Coulter, R. C. Welsh, and T. E. Chupp, Brain MRI with laser-polarized ^{129}Xe, *Magn. Reson. Med.* **38,** 695–698 (1997).
14. S. Peled, F. A. Jolesz, C. H. Tseng, L. Nascimben, M. S. Albert, and R. L. Walsworth, Determinants of tissue delivery for ^{129}Xe magnetic resonance in humans, *Magn. Reson. Med.* **36,** 340–344 (1996).
15. I. Solomon, Relaxation processes in a system of two spins, *Phys. Rev.* **99,** 559–565 (1955).
16. G. Navon, Y. Q. Song, T. Room, S. Appelt, E. Taylor, and A. Pines, Enhancement of solution NMR and MRI with laser polarized xenon, *Science* **271,** 1848–1851 (1996).
17. Y. Q. Song, B. M. Goodson, R. E. Taylor, D. D. Laws, G. Navon, and A. Pines, Selective enhancement of NMR signals for α-cyclodextrin with laser polarized xenon, *Angew. Chem. Int. Ed. Engl.* **36,** 2368–2370 (1997).
18. N. D. Bhaskar, T. McClelland, and W. Happer, Efficiency of spin exchange between rubidium spins and ^{129}Xe nuclei in a gas, *Phys. Rev. Lett.* **49,** 25–28 (1982).
19. W. Happer, E. Miron, S. Schaefer, D. Schreiber, W. A. Van Wijngaarden, and X. Zeng, Polarization of the nuclear spins of noble-gas atoms by spin exchange with optically pumped alkali-metal atoms, *Phys. Rev. A* **29,** 3092–3110 (1984).
20. T. G. Walker and W. Happer, Spin-exchange optical pumping of noble-gas nuclei, *Rev. Mod. Phys.* **69,** 629–642 (1997).
21. G. D. Cates, R. J. Fitzgerald, A. S. Barton, P. Bogorad, M. Gatzke, N. R. Newbury, and B. Saam, Rb–^{129}Xe spin-exchange rates due to binary and three-body collisions at high Xe pressures, *Phys. Rev. A* **45,** 4631–4639 (1992).
22. C. J. Jameson, A. K. Jameson, and J. K. Hwang, Nuclear spin relaxation by intermolecular magnetic dipole coupling in the gas phase. ^{129}Xe in oxygen, *J. Chem. Phys.* **89,** 4074–4081 (1988).
23. H. C. Torrey, Chemical shift and relaxation of Xe^{129} in xenon gas, *Phys. Rev.* **130,** 2306–2312 (1963).
24. B. Driehuys, G. D. Cates, and W. Happer, Surface relaxation mechanisms of laser-polarized ^{129}Xe, *Phys. Rev. Lett.* **74,** 4943–4946 (1995).
25. X. Zeng, E. Miron, W. A. Van Wijngaarden, D. Schreiber, and W. Happer, Wall relaxation of spin polarized ^{129}Xe nuclei, *Phys. Lett. A* **96,** 191–194 (1983).
26. R. F. Tilton, Jr., and I. D. Kuntz, Nuclear magnetic resonance studies of ^{129}Xe with myoglobin and hemoglobin, *Biochemistry* **21,** 6850–6857 (1982).
27. K. Bartik, M. Luhmer, S. J. Heyes, R. Ottinger, and J. Reisse, Probing molecular cavities in α-cyclodextrin solutions by xenon NMR, *J. Magn. Reson. B* **109,** 164 (1995).
28. T. K. Hitchens and R. G. Bryant, Noble-gas relaxation agents, *J. Magn. Reson.* **124,** 227 (1997).
29. B. Driehuys, G. D. Cates, E. Miron, K. Sauer, D. K. Walter, and W. Happer, High-volume production of laser-polarized ^{129}Xe, *Appl. Phys. Lett.* **69,** 1668–1670 (1996).
30. M. Gatzke, G. D. Cates, B. Driehuys, D. Fox, W. Happer, and B. Saam, Extraordinarily slow nuclear spin relaxation in frozen laser-polarized ^{129}Xe, *Phys. Rev. Lett.* **70,** 690–693 (1993).
31. A. Rossi-Fanelli, E. Antonini, and A. Caputo, Studies on the structure of hemoglobin. I. Physicochemical properties of human globin, *Biochim. Biophys. Acta* **30,** 608–615 (1958); T. Yonetani, Studies on cytochrome *c* peroxidase, *J. Biol. Chem.* **242,** 5008–5013 (1967).